

Design of experiments assisted the development of inclusion complexes of ramipril using hydrophilic carriers for enhancement of solubility and dissolution rate

Azeez Mohammad^{1*}, Sumer Singh¹, Suryakanta Swain², Rabinarayan Parhi³

¹School of Pharmacy and Medical Sciences, Singhania University, Pachheri Bari, Jhunjhunu, Rajasthan, India, ²School of Pharmacy and Paramedical Sciences, K.K. University, Berauti, Bihar Sharif, Nalanda, Bihar, India, ³Department of Pharmaceutical Sciences, Susruta School of Medical and Paramedical Sciences, Assam University (Central University), Silchar, Assam, India

The goal of the present study was to develop inclusion complexes and polymers dispersions of ramipril prepared by physical mixing, kneading, co-evaporation, and solvent evaporation methods to enhance drug solubility and dissolution rate, and thereby to reduce drug dose and side effects using selected hydrophilic carriers such as β -CD, PVP-K25, PEG 4000, and HPMC K100M. The prepared formulations were characterized for solubility and in-vitro drug release studies. The systematic optimization of formulations was performed using I-Optimal experimental design by selecting factors such as type of carriers (X1), drug: carrier ratio (X2), and method of preparation (X3), and response variables including percent yield (Y1), solubility (Y2), Carr's index (Y3) and drug release in 30 min (Y4). Mathematical modeling was carried out using a quadratic polynomial model. The inclusion complex formulation (F27) was selected as an optimized batch by numerical desirability function and graphical optimization with the help of design space. The inclusion complex prepared by the co-evaporation method showed maximum drug solubility and released in pH 6.8 phosphate buffer compared to pure and other formulations. The inclusion complex is a feasible approach to improve the solubility, dissolution rate, bioavailability, and minimization of drugs' gastrointestinal toxicity upon oral administration of ramipril.

Keywords: Ramipril. β -cyclodextrin. Inclusion complexes. I-optimal design. Solubility. X-RD. *In-vitro* drug release.

INTRODUCTION

Hypertension is the sustained increase in blood pressure greater than 140/90 mmHg. It is the most common cardiovascular disease, and its prevalence increases with advancing age (Chobanian *et al.*, 2003). A recent report suggested that the global prevalence of hypertension is approximately 1 billion in population, and it causes around 7.1 million deaths per year (Alderman, 2007). Thus, cost-effective treatment of hypertension is of social significance

(Parhi, Suresh, Pattnaik, 2016). Out of various classes of antihypertensive drugs, including calcium channel blockers, β -blockers, angiotensin-converting enzyme (ACE) inhibitors, angiotensin II receptor antagonists, and thiazide diuretics, ACE inhibitors have proven to be very useful for the treatment of hypertension due to their efficacy and lower adverse effects. Besides, this class of drugs provides particular advantages in treating patients with diabetes as they slow down the development and progression of diabetic glomerulopathy, and they also slow the progression of glomerulosclerosis (a chronic renal disease). Ramipril is one of the potent ACE inhibitors which inhibits the ACE and thereby reduces the level of angiotensin II (an essential regulator of cardiovascular

*Correspondence: A. Mohammad. School of Pharmacy and Medical Sciences. Singhania University, Pachheri Bari, Jhunjhunu. Rajasthan-333515, India. Phone: +91-9885397747. E-mail: azeezmohammadphdscholar@gmail.com. ORCID: <https://orcid.org/0000-0002-4501-1323>

function). Poor water solubility (sparingly soluble in water) is the primary concern associated with ramipril, which lowers the oral bioavailability to a mere 28-35%. Besides, it undergoes significant first-pass metabolism in the liver to produce active metabolite ramiprilate (Mukherjee, Ray, Thakur, 2009).

Oral drug delivery has many advantages over other routes of drug delivery as it provides the simplest and easiest way of drug administration. It also provides benefits such as more excellent drug stability, accurate dosing, cheaper cost of production, and patient convenience (Youn *et al.*, 2006; Sugawara *et al.*, 2005). However, poorly water-soluble drugs have many difficulties in developing pharmaceutical dosage forms due to their slow dissolution rate and subsequent poor absorption and bioavailability. Therefore, improving drug solubility in the aqueous medium, thereby its oral bioavailability, remains an essential aspect of oral dosage development. There are numerous approaches reported and have been used to enhance the solubility of poorly soluble drugs, including salt formation, particle size reduction, solid dispersion, inclusion complexes, co-precipitation and spray drying have been utilized for the enhancement of gastrointestinal absorption of poorly water-soluble drugs (Kedzierewicz, Huffman, Maincent, 1990; Kislalioglu *et al.*, 1991; Kim *et al.*, 1994; Duchene, Wouessidjewe, 1990).

Cyclodextrin is an oligomer of glucose that is produced from the enzymatic modification of starch. An inclusion complex is formed when the hydrophobic inner cavity interacts with a moiety of the drug by non-covalent forces (Yoshida *et al.*, 1988). Formulators have utilized cyclodextrin and its derivatives to increase solubility, stability, and bioavailability of poorly water-soluble drugs to reduce side effects and toxicity of drugs (Szejtli, 1991; Duchene, Wouessidjewe, 1990). The highly water-soluble 2-hydroxypropyl β -cyclodextrin (2-HP β -CD) is a commercially available complexing agent of various compounds due to its higher aqueous solubility and lower toxicity compared to the natural counterpart. Therefore, it is interesting to investigate the solubility and dissolution rate of inclusion complexes containing poorly water-soluble drugs to simultaneously improve bioavailability and reduce gastrointestinal toxicity when given orally (Nambu *et al.*, 1978).

Systematic development of the pharmaceutical dosage forms is highly essential as per the current regulatory requirement by ICH Q8 and US-FDA. In this regard, the Quality by Design (QbD) approach is considered one of the highly efficient tools for product development with predefined objectives (Swain *et al.*, 2012). The application of QbD principles requires experimental designs, which help rationalize the formulation attributes and process parameters. Several literature reports have been published on the application of innovative techniques to develop F27 drug formulation. Thus, the present research studies also involved implementing an I-optimal design for optimizing the inclusion of complex formulations using the selected factors and response variables (Komati *et al.*, 2018)

Based on the above fact, this study aims to prepare and characterize the drug-loaded inclusion complexes, using β -cyclodextrin, PVP-K25, PEG 4000, and HPMC K100M as hydrophilic carriers made by physical mixing, kneading, co-evaporation, and solvent evaporation methods to improve the solubility and dissolution rate of ramipril, which would increase the biological activities. They may enhance drug absorption (Muller, Mader, Gohla, 2000).

MATERIAL AND METHODS

Ramipril was a gift sample from M/s Ranbaxy Labs. Ltd., Gurgaon, Haryana, India. β -cyclodextrin and PVP-K25 were procured from Yarrow Chem Products, Mumbai, India. PEG 4000 and HPMC K100M were obtained from M/s Loba Chem Pvt. Ltd., Mumbai, India. All other chemicals and reagents used in the experiment were of analytical reagent grade, and the Double distilled water was used throughout the study.

Solubility studies

According to the method described by Higuchi and Connors (1965), solubility studies were carried out with minor modifications. Excess amounts of drugs were added to distilled water containing various concentrations of β -cyclodextrin. The resulted suspensions were sonicated and vortexed and then placed in a constant temperature water

bath at 25°C for 6 days. The parafilm was used to cover the top of the suspension to prevent evaporation. Samples were collected and filtered through a membrane filter (0.45µm). The drug concentration was analyzed using UV-Visible spectrophotometry (UV-Visible spectrophotometer 1700, Shimadzu, Japan) at wavelength λ_{\max} 231 nm after proper dilution (Higuchi, Connors, 1965).

Micromeritic properties

The flowability of ramipril was investigated by determining the angle of repose, bulk density, Carr's index, and Hausner's ratio. The angle of repose was established by the fixed height method ($\tan \theta = h/r$). Ramipril was tapped using USP tapped density tester (Electro labs, ETD 1020, Mumbai, India) 100 times in a cylinder, and the change in volume was measured. Carr's index and Hausner's ratio were calculated using equations 1 and 2 (Rao *et al.*, 2011).

$$\text{Carr's Index (\%)} = \frac{DB - DT}{DB} \times 100 \quad \text{Eq. (1)}$$

$$\text{Hausner's ratio} = \frac{DB}{DT} \quad \text{Eq. (2)}$$

Where, DB is poured or bulk density, DT is tapped density.

Fourier Transform Infrared (FT-IR)

FT-IR spectra of pure drug, β -CD, and F27 inclusion complex were recorded on the FT-IR spectrophotometer (Shimadzu, Tokyo, Japan) using the KBr disc method. The instrument was operated under a dry air purge, and the scans were collected at a scanning speed of 2 mm/s with a resolution of 4 cm^{-1} over the region of 4000–400 cm^{-1} . The scans were evaluated for the presence of principal drug peaks, the shifting and masking of drug peaks due to β -CD, and new heights (Swain *et al.*, 2014).

Differential scanning calorimetric (DSC)

The DSC curves of pure drug, β -CD, and F27 inclusion complex were recorded on the SII EXSTAR DSC 6220 model of differential scanning calorimeter. The

thermal behavior was studied by heating all samples (10 mg) in sealed aluminum pans, using alumina powder as a reference, over a temperature range of 30 to 300°C at a heating rate of 10°C/min. Dry nitrogen was used as a purge gas. The results of pure materials and solid systems were evaluated for shift and change in the intensity of peaks (Swain *et al.*, 2014).

X-ray diffraction (X-RD) studies

Powder X-ray diffraction patterns were performed using the Phillips P Analytical X'PertPRO powder X-ray diffractometer. The scanning rate employed was 1°/min, and the samples were analyzed between 2 θ angles of over 10–80. The powder diffraction patterns of pure drug, β -CD, and F27 inclusion complex were recorded.

Preparation of inclusion complexes, and polymers dispersions

The material combination of ramipril and the selective carriers prepared by mixing of the drug (ramipril) with the carrier in the molar ratio of (1:1), (1:2), and (1:4) in a mortar and pestle for about 1h with constant trituration and passed through sieve no. # 100. Likewise, in the case of the kneading method, a drug with selected hydrophilic carriers of molar ratios (1:1), (1:2), and (1:4) were taken. First, the hydrophilic carrier is added to the mortar, and then a small quantity of 50% methanol is added while triturating to get slurry-like consistency. After that, the drug was slowly incorporated into the slurry, and trituration continued for 1 h. The slurry is then air-dried at 25°C for 24 h, pulverized, and passed through sieve no. #100. In the case of the co-evaporation method, the drug with the equimolar ratios of hydrophilic carriers (1:1), (1:2), and (1:4) along with 50% aqueous ethanol was added to prepare the inclusion complexes and polymers dispersions of ramipril. The solution was stirred at 100 rpm till a clear solution was observed, and the obtained solution was evaporated under vacuum at a temperature of 45°C. The solid residues were further dried completely at 45°C temperature for 48 h. The dried inclusion complex and polymers dispersions were pulverized into fine powder and sieved through sieve no. 100 and stored in a desiccator

before their use in further studies. Finally, in the solvent evaporation method, drug, and selected carriers were used in different ratios of 1:1, 1:2, and 1:4 and dissolved in methanol (20 ml), with continuous stirring till the solvent

was removed by evaporation. The prepared complexes and polymers dispersions were pulverized and sifted through sieve no. 100 and stored in a desiccator until further studies (Table I).

TABLE I - Formulation design of ramipril inclusion complexes prepared by physical mixture, kneading, co-evaporation and solvent evaporation methods

Formulation code (F0- F12)	Drug: polymer ratio (Physical mixing Method)	Formulation code (F13-F24)	Drug: polymer ratio (Kneading method)	Formulation code (F25-F36)	Drug: polymer ratio (Co-evaporation method)	Formulation code (F37-F48)	Drug: polymer ratio (Solvent evaporation method)
F0	Pure drug (1 part)						
F1	Drug : β -CD (1:1)	F13	Drug : β -CD (1:1)	F25	Drug : β -CD(1:1)	F37	Drug : β -CD (1:1)
F2	Drug : β -CD (1:2)	F14	Drug : β -CD(1:2)	F26	Drug : β -CD(1:2)	F38	Drug : β -CD (1:2)
F3	Drug : β -CD (1:4)	F15	Drug : β -CD(1:4)	F27	Drug : β -CD(1:4)	F39	Drug : β -CD (1:4)
F4	Drug : PEG 4000 (1:1)	F16	Drug : PEG 4000(1:1)	F28	Drug : PEG 4000(1:1)	F40	Drug : PEG 4000 (1:1)
F5	Drug : PEG 4000 (1:2)	F17	Drug : PEG 4000(1:2)	F29	Drug : PEG 4000(1:2)	F41	Drug : PEG 4000 (1:2)
F6	Drug : PEG 4000 (1:4)	F18	Drug : PEG 4000(1:4)	F30	Drug : PEG 4000(1:4)	F42	Drug : PEG 4000 (1:4)
F7	Drug : PVP-K25 (1:1)	F19	Drug : PVP-K25(1:1)	F31	Drug : PVP-K25(1:1)	F43	Drug : PVP-K25 (1:1)
F8	Drug : PVP-K25 (1:2)	F20	Drug : PVP-K25(1:2)	F32	Drug : PVP-K25(1:2)	F44	Drug : PVP-K25 (1:2)
F9	Drug : PVP-K25 (1:4)	F21	Drug : PVP-K25(1:4)	F33	Drug : PVP-K25(1:4)	F45	Drug : PVP-K25 (1:4)
F10	Drug : HPMC K100M (1:1)	F22	Drug : HPMCK100 M (1:1)	F34	Drug : HPMC K100 M (1:1)	F46	Drug : HPMC K100 M (1:1)
F11	Drug : HPMC K100M (1:2)	F23	Drug : HPMC K100 M(1:2)	F35	Drug : HPMC K100 M(1:2)	F47	Drug : HPMC K100 M (1:2)
F12	Drug : HPMC K100M (1:4)	F24	Drug : HPMC K100 M(1:4)	F36	Drug : HPMC K100 M(1:4)	F48	Drug : HPMC K100 M (1:4)

Systematic optimization using I-optimal experimental design

I-optimal response surface design was used for the optimization of the factors related to the formulation of inclusion complexes and polymers dispersions where the type of carrier (X1), drug: carrier ratio (X2), and method of preparation (X3) were selected as the factors. A total of

19 formulation trials were obtained as per the I-Optimal experimental design, which was evaluated for various response variables such as percent yield (Y1), solubility (Y2), Carr's index (Y3), and drug release in 30 min (Y4). The optimization data analysis was carried out by mathematical modeling with the help of multiple linear regression analysis (MLRA). The quadratic polynomial model was selected by considering the main effects and the

interaction effects of the factors. Model fitness suitability was evaluated using p-value, coefficient of correlation (R²), and lack of fit. Response surface analysis was performed using 3D and 2D plots for understanding the relationship and interactions between the studied factors on the response variables. The F27 formulation was selected by numerical optimization and desirability function by “trading-off” the elements for attaining desired goals, i.e., maximization of percent yield of inclusion complexes, solubility, and drug release and minimization of carr’s index for the prognosis of the F27 stable inclusion complex formulation. Also, the graphical optimization was carried out for demarcating the F27 formulation in the design space region (Aleksandra *et al.*, 2019).

CHARACTERIZATION OF INCLUSION COMPLEXES, AND POLYMERS DISPERSIONS

Solubility analysis of complexes, and polymers dispersions

Solubility analysis was carried out for the prepared complexes and polymers dispersions by taking the drug and selected hydrophilic carriers (β -CD, PVP-K25, PEG 4000, and HPMC K100M) in different ratios, such as 1:1, 1:2, and 1: 4. To this, 10 ml of phosphate buffer pH 6.8 was added and shaken for 48 h in a rotary shaker. After that, the solution was filtered by using Whatman filter paper. From the filtrate, 1ml was taken, and the absorbance was measured at the wavelength of λ_{max} 231 nm using a UV-Visible spectrophotometer (Swain *et al.*, 2019).

Percentage yield

The percentage yields of all the prepared complexes and polymers dispersions were calculated using the weight of finally dried compounds concerning the initial quantity of drug and total hydrophilic carriers used to prepare complexes. Percentage production yield is calculated by using equation 3 (Swain *et al.*, 2019).

$$\text{Percentage yield} = \frac{\text{Practical mass (Prepared complexes)}}{\text{Theoretical mass (Polymer : drug)}} \times 100$$

Eq. (3)

Drug content

100 mg drug equivalent weight of inclusion complexes and polymers dispersions were taken correctly, powdered in a mortar and pestle, and suspended in a volumetric flask (100 mL capacity) containing 100 mL of phosphate buffer pH 6.8. The resultant dispersion was kept for 2 h in a mechanical shaker to extract the drug, and then it was filtered through a Whatman filter paper. The drug content was determined spectrophotometrically (UV-Visible spectrophotometer 1700, Shimadzu, Japan) after suitable dilution at λ_{max} 231 nm using a regression equation derived from the standard graph ($Y = 0.010X - 0.011$) (Swain *et al.*, 2014).

Micromeritics properties

The flowability of prepared complexes and polymers dispersions were investigated by determining the angle of repose, bulk density, tapped density, carr’s index, Hausner’s ratio, and flow rate.

Angle of repose

The angle of repose is defined as the maximum angle possible between the surface of the pile of the prepared complexes and the horizontal plane. The angle of repose was determined by using the fixed funnel method. Complexes and polymers dispersions were poured from a funnel raised vertically until a maximum cone height (h) was obtained. The radius of the pile of complexes or polymers dispersions (r) was measured. The repose angle was calculated using the following formula given in equation 4 (Parhi, Reddy, Swain, 2019).

$$\text{Tan } \theta = \frac{(h)}{(r)}$$

Eq. (4)

Where, h= height of pile (cm), r = radius of the base of the pile (cm), θ = angle of repose ($^{\circ}$).

Bulk density

Apparent bulk density was obtained by pouring prepared complexes, and polymers dispersions into a graduated cylinder and measuring the volume and weight “as it is” by using the formula given in equation 5 (Parhi, Reddy, Swain, 2019).

$$\text{Bulk density} = \frac{\text{Mass}}{\text{Bulk volume}} \quad \text{Eq. (5)}$$

Tapped density

It was determined by placing a graduated cylinder containing a known mass of complexes or polymers dispersions. The complexes were tapped using USP Tapped Density Tester (Electrolabs, Mumbai) 1000 times in a cylinder, and the volume change was measured on the mechanical tapping apparatus. The tapped density is calculated using the formula given in equation 6 (Parhi, Reddy, Swain, 2019).

$$\text{Tapped density} = \frac{\text{Mass}}{\text{Tapped volume}} \quad \text{Eq. (6)}$$

Compressibility index (Carr's index)

Carr's index is calculated using the formula given in equation 7 (Parhi, Reddy, Swain, 2019).

$$\text{Carr's index} = 1 - \frac{\text{Tapped Density}}{\text{Untapped Density}} \times 100 \quad \text{Eq. (7)}$$

Hausner's ratio

Hausner's ratio is a number that is correlated to the flowability of a powder or granular materials. It is calculated by using the formula given in equation 8 (Parhi, Reddy, Swain, 2019).

$$\text{Hausner's ratio} = \frac{\text{Tapped Density}}{\text{Untapped Density}} \quad \text{Eq. (8)}$$

Hausner's ratio is used in a wide variety of industries as an indication of the flowability of a powder. A Hausner's ratio value greater than 1.25 is considered to be an indication of poor flowability. < 1.25 – good flow = 20% Carr's index, >1.25 – poor flow = 33 % Carr's index.

In-vitro drug release study

The release of drug from prepared complexes, and polymers dispersions were studied using the USP II dissolution apparatus (DBK Instruments, Mumbai). The formulations are equivalent to 100 mg of ramipril were taken and enclosed in the hard gelatin capsules and immersed in the 900 mL of phosphate buffer pH 6.8 for 1h at 37±0.5°C and was rotated at 100 rpm. Sample aliquots of 5 ml were withdrawn periodically from dissolution fluids. Every time a 5 mL of fresh medium, maintained at 37±0.5°C, was added immediately after removing each test aliquot to keep the sink condition. The dissolution test of all selected formulations was performed in triplicate (Ekambaram, Abdul, 2011). To establish the mechanism of release of the drug from the prepared complexes, and polymers dispersions, the experimental data were fitted to different kinetic models like zero order, first order, Higuchi, and Korsmeyer-Peppas's model. The Higuchi model was used to determine whether the release of drug from inclusion complexes or polymers dispersions follows the diffusion mechanism or not. In contrast, Korsmeyer-Peppas's model was used to identify the diffusion mechanism type and find more than one kind of release phenomenon.

Korsmeyer-Peppas's equation is shown in equation 9.

$$\frac{M_t}{M_\infty} = Kt^n \quad \text{Eq. (9)}$$

Where $M_t / (M_\infty)$ is the fractional drug release in time 't.' K =rate constant incorporating, n =diffusional release exponent indicative of release mechanism.

RESULTS AND DISCUSSION

The research was undertaken to prepare and characterize the ramipril-loaded inclusion complexes and

polymers dispersions by physical mixing, kneading, co-evaporation, and solvent evaporation methods using β -CD PVP-K25, PEG 4000, and HPMC K100M as hydrophilic carriers. Table I indicated the formulations from F0 (Pure drug) to F48.

Fourier transform infrared (FT-IR) spectroscopy

FT-IR spectra of the pure drug (ramipril) showed the characteristic peaks for C-H stretching (Alkane and alkene) at 2900.82 cm^{-1} and 3022.85 cm^{-1} , C-H bending (Aromatic) at 751.43 cm^{-1} , C=C stretching (Alkyne) at 2124.99 cm^{-1} , C=C stretching (Aromatic) at 1454.79 cm^{-1} ,

OH stretching (free) at 3629.75 cm^{-1} , C-O stretching (Phenol) at 1401.47 cm^{-1} , C-O stretching (Alcohol) at 1224.01 cm^{-1} , N-H bending at 3436.39 cm^{-1} , C-N vibrations at 1021.53 cm^{-1} , C=N stretching (aromatic) at 1650.72 cm^{-1} and S-H stretching (aromatic) at 2579.11 cm^{-1} which were compared with the peaks of a physical mixture of drug with β -CD and F27 batch. The FT-IR spectra of drug and β -CD combination confirmed that there was neither any shift in the wavenumbers of the peaks nor the intensity, indicating the absence of interaction between drug and β -CD. This was attributed to the encapsulation of drug within β -CD. Hence, the drug and β -CD were compatible with each other (Figure 1).

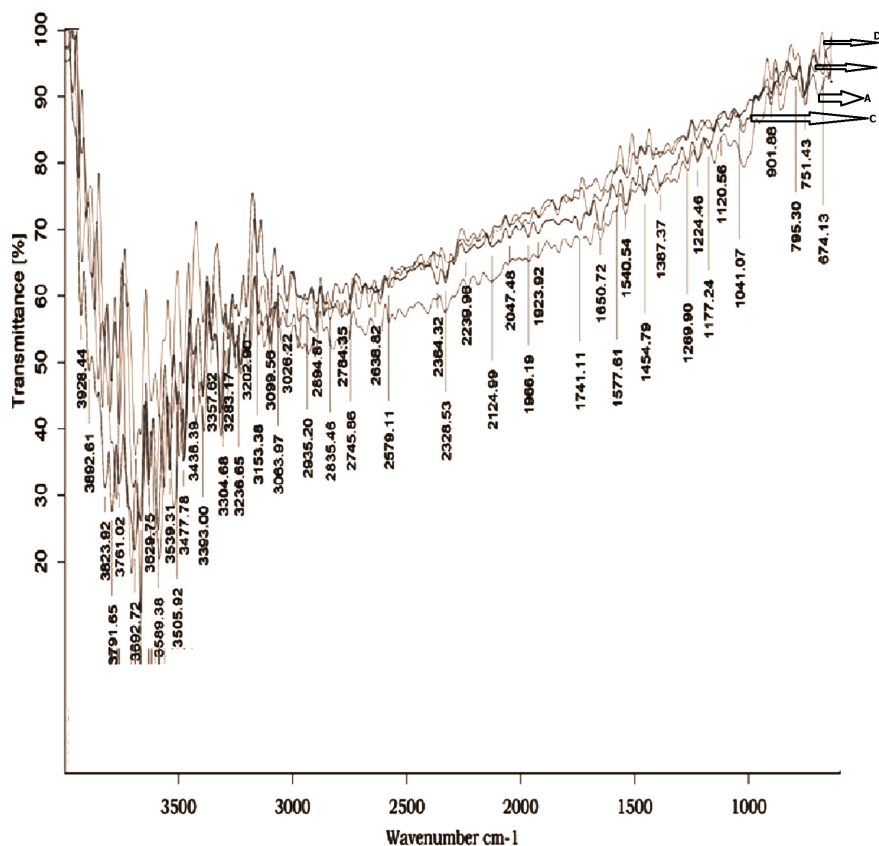


FIGURE 1 - FT-IR spectra of pure drug (A), β -CD (B), physical mixture of drug and β -CD (C) and F27 formulation (D).

Differential scanning calorimetry (DSC)

DSC curves of pure ramipril, β -CD, physical mixture, and F27 formulation are shown in Figure 2.

DSC thermograms of the pure drug and β -CD showed endothermic peaks at 107.04°C and 112.29°C, respectively, indicating their melting points. The DSC thermogram of the physical mixture demonstrated a shifted peak to a

lower temperature (105.96°C) with reduced intensity. However, the F27 formulation exhibited the endothermic

peak at 107.76°C. The former result may be attributed to the complete complexation of ramipril with the β -CD.

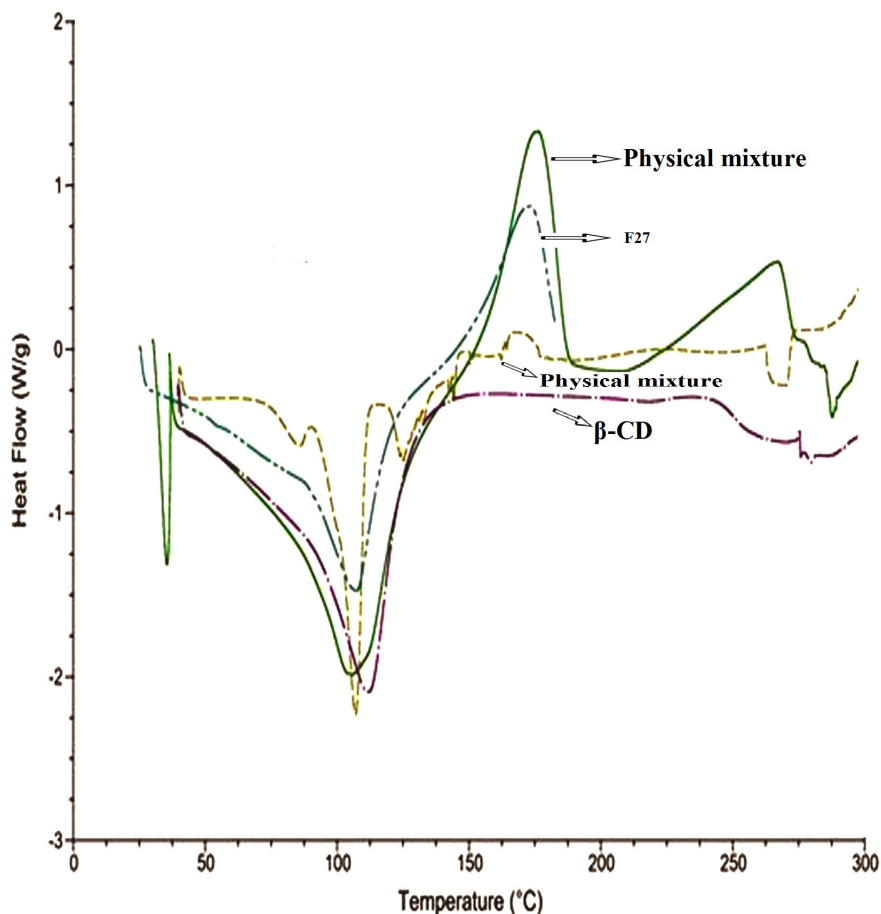


FIGURE 2 - DSC thermogram of ramipril; β -CD; physical mixture drug and β -CD, and F27 formulation.

X-Ray Diffraction (X-RD)

The powder X-ray diffraction patterns of the pure drug (ramipril), β -CD, and optimized formulation (F27) are illustrated in Figure 3. The sharp peaks of the pure drug appeared in the 2θ range of 10–80, indicating that it was crystalline material. The highest peak intensity of ramipril was 80627 at 17.8447. In the case of β -CD and F27 formulation, the highest peak intensity was 28282 at

12.8448 and 47564 at 12.3304, respectively. The reduction in intensity and sharpness of F27 formulation peaks could be attributed to the entrapment of ramipril into the β -CD cavity through the formation of the inclusion complex. However, the P-XRD pattern of the F27 optimized inclusion complex exhibited a halo shape with less intense and denser peaks compared to a pure drug, and β -CD indicated the decrease in crystallinity or partial amorphization of the drug in its complex form (Patra *et al.*, 2015).

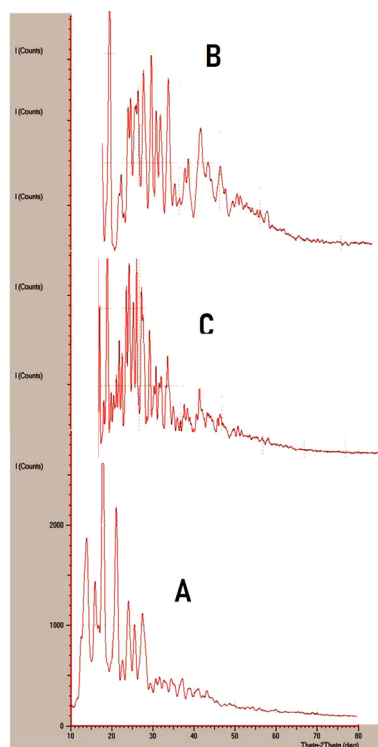


FIGURE 3 - X-RD study of pure drug (A); β -CD (B) and F27 formulation (C).

Formulation of ramipril inclusion complexes, and polymers dispersions

Table I showed the formulation design of ramipril inclusion complexes and polymers dispersions prepared by physical mixing, kneading, co-evaporation, and solvent evaporation.

Systematic optimization using experimental design

Table II summarizes the design matrix indicating the factors and their levels investigated during the formulation optimization study. Among the three factors selected, the type of carrier and method of preparation used to develop the inclusion complexes or polymers dispersions were taken as categorical factors at three levels and four levels, respectively. In contrast, the drug: carrier ratio was selected as the numerical factor at three levels. A total of 19 trial formulations were obtained and evaluated for the desired response variables.

TABLE II - List of factors and response variables selected for response surface optimization

Name of the factors	Type of factors	Factors Continuity	Levels of the factors			
			L1	L2	L3	L4
X1: Type of carrier	Categorical	Nominal	PEG 4000	PVP-K25	β -CD	-
X2: Drug: carrier ratio	Numerical	Discrete	1:1	1:2	1:4	-
X3: Method of preparation	Categorical	Nominal	PM	KM	CM	SEM

PM: Physical mixing method; KM: Kneading method; CM: Co-evaporation method; SEM: Solvent evaporation method

Mathematical model development

The optimization was carried out by establishing the cause-and-effect relationship among the studied factors and responses. The best-fitting with the quadratic polynomial model with the model equation (Eq. 10) for all the responses variables were considered. All the responses indicated an excellent model fitting with statistical significance for the experimental data (P

< 0.05) and the model coefficient of correlation (R²) ranging between 0.9892 and 0.9995. Supplementary data Table S1-S4 provides the details of ANOVA for all the response variables along with the model equation and vital statistical parameters.

$$Y = b_0 + b_1X_1 + b_2X_2 + b_3X_1^2 + b_4X_2^2 + b_5X_1X_2 + b_6X_1^2X_2 + b_7X_1X_2^2$$

Eq. (10)

TABLE S1 - ANOVA table for the response variable percent yield along with the polynomial equation

ANOVA for Response Surface Reduced Quadratic model						
Source	Sum of Squares	df	Mean Square	F Value	p-value Prob > F	
Model	3160.49	11	287.32	4.09	0.0362	Significant
A-Type of carrier	2598.10	1	2598.10	37.02	0.0005	
B-Drug: Carrier ratio	67.60	1	67.60	0.96	0.3591	
C-Method of preparation	32.22	3	10.74	0.15	0.9245	
AB	18.00	1	18.00	0.26	0.6281	
AC	392.47	3	130.82	1.86	0.2239	
A ²	8.10	1	8.10	0.12	0.7440	
B ²	147.00	1	147.00	2.09	0.1911	
Residual	491.30	7	70.19			
Lack of Fit	366.30	5	73.26	1.17	0.5200	Not significant
Pure Error	125.00	2	62.50			
Cor Total	3651.79	18				

$$Y1 \text{ (Percent yield)} = 62.28 + 14.5 * X1 - 2.6 * X2 - 0.67 * X3[1] + 3.52 * X3[2] - 3.37 * X3[3] + 1.5 * X1 X2 - 3 * X1 X3[1] + 10.5 * X1 X3[2] + 0.5 * X1 X3 AC[3] - 1.8 * X1^2 + 7 * X1^2$$

TABLE S2 - ANOVA table for the response variable solubility along with the polynomial equation

ANOVA for Response Surface Reduced Cubic model						
Analysis of variance table [Classical sum of squares - Type II]						
Source	Sum of Squares	df	Mean Square	F Value	p Value Prob > F	
Model	9161.84	15	610.79	429.46	0.0002	Significant
A-Type of carrier	646.67	1	646.67	454.69	0.0002	
B-Drug: Carrier ratio	672.40	1	672.40	472.78	0.0002	
C-Method of preparation	1316.31	3	438.77	308.51	0.0003	
AB	484.00	1	484.00	340.31	0.0003	
AC	4146.36	3	1382.12	971.80	< 0.0001	
BC	974.47	3	324.82	228.39	0.0005	
A ²	87.02	1	87.02	61.19	0.0043	
B ²	44.08	1	44.08	31.00	0.0114	
AB ²	533.33	1	533.33	375.00	0.0003	
Residual	4.27	3	1.42			
Lack of Fit	4.27	1	4.27			
Pure Error	0.000	2	0.000			
Cor Total	9166.11	18				

$$Y2 \text{ (Solubility)} = 50.45 + 16.31 * X1 + 6.12 * X2 - 1.91 * X3 [1] - 12.51 * X3 [2] - 5.31 * X3 [3] + 11 * X1X2 + 13.19 * X1X3[1] - 15.15 * X1X3[2] + 22.19 * X1X3 [3] + 10.37 * X2X3 [1] - 6.62 * X2X3[2] + 9.38 * X2X3[3] + 5.9 * X1^2 + 3.83 * X2^2 - 20 * X2X3^2$$

TABLE S3 - ANOVA table for the response variable Carr's index along with the polynomial equation

ANOVA for Response Surface Reduced Cubic model						
Analysis of variance table [Classical sum of squares - Type II]						
Source	Sum of Squares	df	Mean Square	F Value	p-value Prob > F	
Model	1879.22	15	125.28	2.60	0.0349	Significant
A-Type of carrier	73.49	1	73.49	1.52	0.3051	
B-Drug: Carrier ratio	275.84	1	275.84	5.71	0.0967	
C-Method of preparation	501.20	3	167.07	3.46	0.1676	
AB	113.85	1	113.85	2.36	0.2222	
AC	121.00	3	40.33	0.84	0.5570	
BC	234.07	3	78.02	1.62	0.3515	
A^2	747.19	1	747.19	15.48	0.0293	
B^2	21.01	1	21.01	0.44	0.5565	
AB^2	113.34	1	113.34	2.35	0.2230	
Residual	144.83	3	48.28			
Lack of Fit	144.83	1	144.83			
Pure Error	0.000	2	0.000			
Cor Total	2024.05	18				

$$Y3 \text{ (Carr's index)} = 43.34 - 1.68 * X1 + 3.91 * X2 - 1.99 * X3 [1] + 8.96 * X3 [2] - 10.4 * X3 [3] + 5.34 * X1X2 - 2.36 * X1X3[1] + 6.08 * X1X3[2] - 0.4 * X1X3[3] + 6.68 * X2X3[1] + 0.46 * X2X3 [2] - 0.02 * X2X3[3] - 17.29 * X1^2 + 2.65 * X2^2 + 9.22 * X1X2^2$$

TABLE S4 - ANOVA table for the response variable drug release in 30 min along with the polynomial equation

ANOVA for Response Surface Reduced Cubic model						
Analysis of variance table [Classical sum of squares - Type II]						
Source	Sum of Squares	df	Mean Square	F Value	p-value Prob > F	
Model	2533.72	15	168.91	9.04	0.0475	Significant
A-Type of carrier	22.77	1	22.77	1.22	0.3503	
B-Drug: Carrier ratio	96.10	1	96.10	5.14	0.1082	
C-Method of preparation	373.01	3	124.34	6.65	0.0770	
AB	16.00	1	16.00	0.86	0.4231	
AC	439.71	3	146.57	7.84	0.0623	
BC	433.28	3	144.43	7.73	0.0635	
A^2	99.22	1	99.22	5.31	0.1046	
B^2	1474.08	1	1474.08	78.87	0.0030	
AB^2	21.33	1	21.33	1.14	0.3637	
Residual	56.07	3	18.69			
Lack of Fit	56.07	1	56.07			
Pure Error	0.000	2	0.000			
Cor Total	2589.79	18				

$$Y4 \text{ (Drug release in 30 min)} = 85.8 - 1.19 * X1 - 2.38 * X2 - 0.86 * X2[1] + 9.34 * X2 [2] + 0.44 * X3[3] + 2 * X1X2 - 0.31 * X1X3 [1] - 10.65 * X1X3 [2] + 1.19 * X1X3 [3] - 3.63 * X2X3 [1] - 3.12 * X2X3 [2] + 12.38 * X2X3 [3] - 6.3 * X1^2 - 22.17 * X2^2 + 4 * X1X2^2$$

Response surface analysis

The response surface analysis was performed with the help of 3D-response surface plots and 2D-contour plots. Figure 4 illustrates the 3D and 2D plots between the selected factors, such as percent yield, solubility, Carr's Index, and drug release in 30 min as the response. Figure 4 (A-B) showed a positive influence of the type of carrier on percent yield, while drug: carrier ratio showed a curvilinear effect on the response variable.

Figure 4 (C-D) showed the negligible impact of the type of carrier on the solubility of the drug, while the drug: carrier ratio showed a profoundly positive influence on solubility. Figure 4 (E-F) showed the curvilinear impact of both types of the carrier and a drug: carrier ratio on Carr's index as the flow property of the prepared formulation. Figure 4 (G-H) showed the negligible influence of the type of carrier, while drug: carrier ratio indicated a curvilinear effect on the drug release in 30 min.

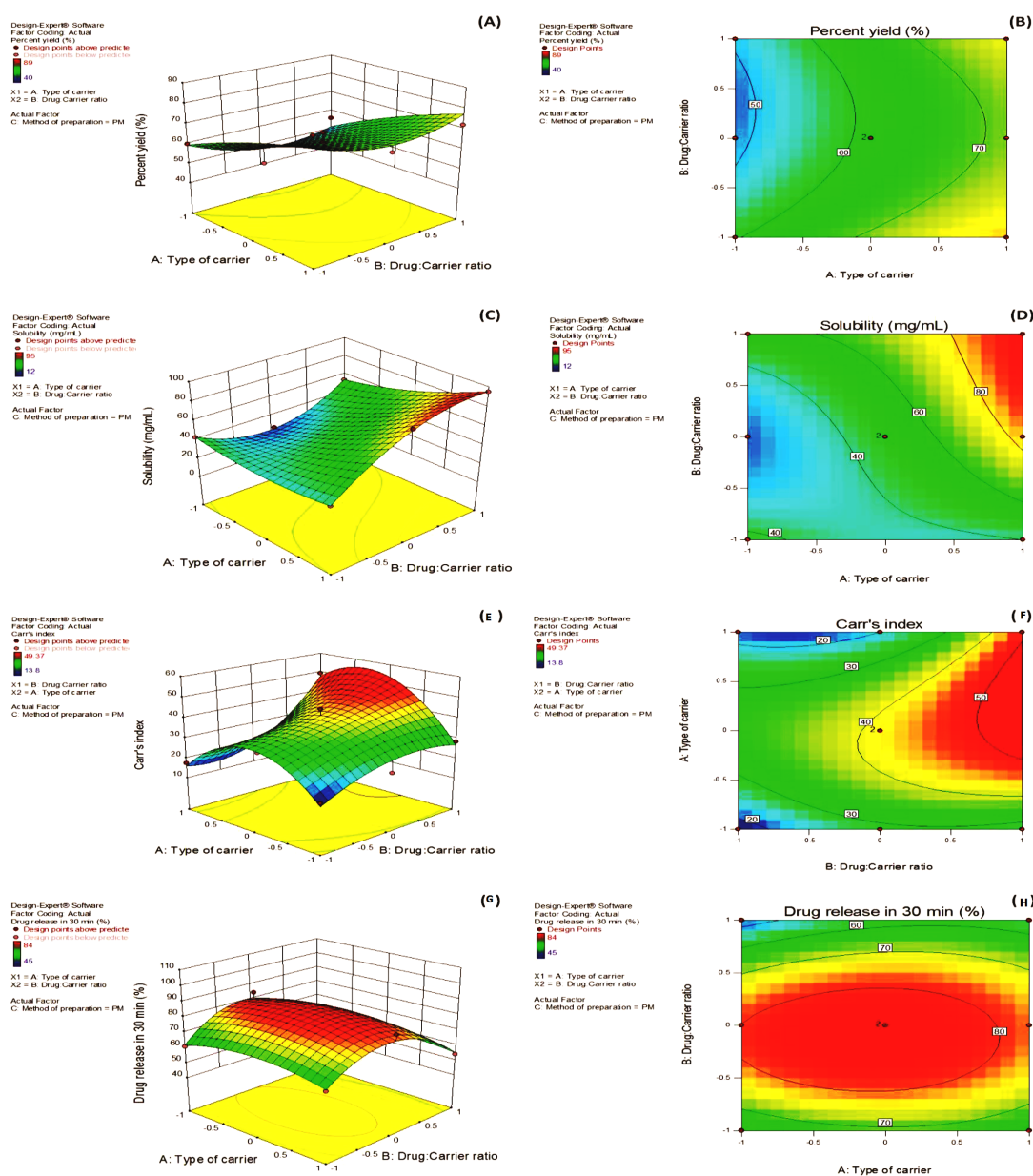


FIGURE 4 - 3D-response surface plots and 2D-contour plots between the selected factors and their effect on various response variables (A-B) percent yield, (C-D) solubility, (E-F) carr's index, (G-H) drug release in 30 min.

Selection of the optimized formulation

Tables III and IV enlist the optimum solutions suggested by the selected experimental design and the design space overlay plot shown in Figure 5. The F27

inclusion complex was formed by drug with the β -CD carrier at a ratio of 1:4 using co-evaporation method was found to be the best, which showed percent yield of 72.1%, maximum drug solubility of 89.9 mg/mL, carr's index of 13.56, and 80% drug release in 30 min.

TABLE III - Design matrix enlisting the experimental trial formulations as per the I-optimal design

Run order	Build type	Factor X ₁ (Type of Carrier)	Factor X ₂ (Drug: Carrier Ratio)	Factor X ₃ (Method of Preparation)	Response 1 (Percent yield)	Response 2 (Solubility in mg/mL)	Response 3 (Carr's Index)	Response 4 (Drug release in 30 min)
7	Model	PEG 4000	1:4	PM	56	54	28.34	45
8	Model	β -CD	1:4	PM	72	95	49.37	54
18	Replicate	PEG 4000	1:2	SEM	62	80	34.49	62
16	Model	β -CD	1:1	SEM	68	52	34.22	67
19	Model	β -CD	1:4	SEM	81	60	38.47	55
14	Model	β -CD	1:2	CM	75	89	16.67	78
2	Model	β -CD	1:1	PM	85	40	17.5	62
1	Model	PEG 4000	1:1	PM	60	43	17.81	61
5	Replicate	PVP-K25	1:2	PM	67	48	44.45	83
13	Model	PEG 4000	1:2	CM	45	12	20.84	78
4	Model	PVP-K25	1:2	PM	62	48	44.45	83
3	Lack of Fit	PEG 400	1:2	PM	40	26	21.88	84
10	Model	β -CD	1:2	KM	89	45	39.4	77
12	Model	PVP-K25	1:1	CM	70	34	28.58	56
9	Model	PEG 400	1:1	KM	50	78	25	82
15	Model	PVP-K25	1:4	CM	56	65	36.37	76
17	Model	PEG 400	1:2	SEM	47	80	34.49	62
11	Model	PEG 400	1:4	KM	42	55	23.08	67
6	Lack of Fit	β -CD	1:2	PM	68	85	13.8	81

PM: Physical mixing method; KM: Kneading method; CM: Co-evaporation method; SEM: Solvent evaporation method

TABLE IV - List of optimum solutions suggested by the I-optimal design by numerical optimization technique

Serial Number	Factor X ₁ (Type of Carrier)	Factor X ₂ (Drug: Carrier Ratio)	Factor X ₃ (Method of Preparation)	Response 1 (Percent yield)	Response 2 (Solubility in mg/mL)	Response 3 (Carr's Index)	Response 4 (Drug release in 30 min)	Desirability
1	0.864	0.990	CM	76.096	94.394	37.052	74.792	1.000
2	0.852	1.000	CM	76.046	93.882	37.543	74.615	1.000
3	0.871	0.981	CM	76.077	94.683	36.668	74.980	1.000
4	0.878	0.991	CM	76.284	94.941	36.818	74.713	1.000

TABLE IV - List of optimum solutions suggested by the I-optimal design by numerical optimization technique

Serial Number	Factor X ₁ (Type of Carrier)	Factor X ₂ (Drug: Carrier Ratio)	Factor X ₃ (Method of Preparation)	Response 1 (Percent yield)	Response 2 (Solubility in mg/mL)	Response 3 (Carr's Index)	Response 4 (Drug release in 30 min)	Desirability
5	0.875	0.974	CM	76.031	94.834	36.386	75.146	1.000
6	0.877	0.998	CM	76.361	94.871	37.069	74.528	1.000

CM: Co-evaporation method

Design-Expert® Software
 Factor Coding: Actual
 Overlay Plot

Percent yield
 Solubility
 Carr's index
 Drug release in 30 min
 ● Design Points

X1 = A: Type of carrier
 X2 = B: Drug:Carrier ratio

Actual Factor
 C: Method of preparation = CM

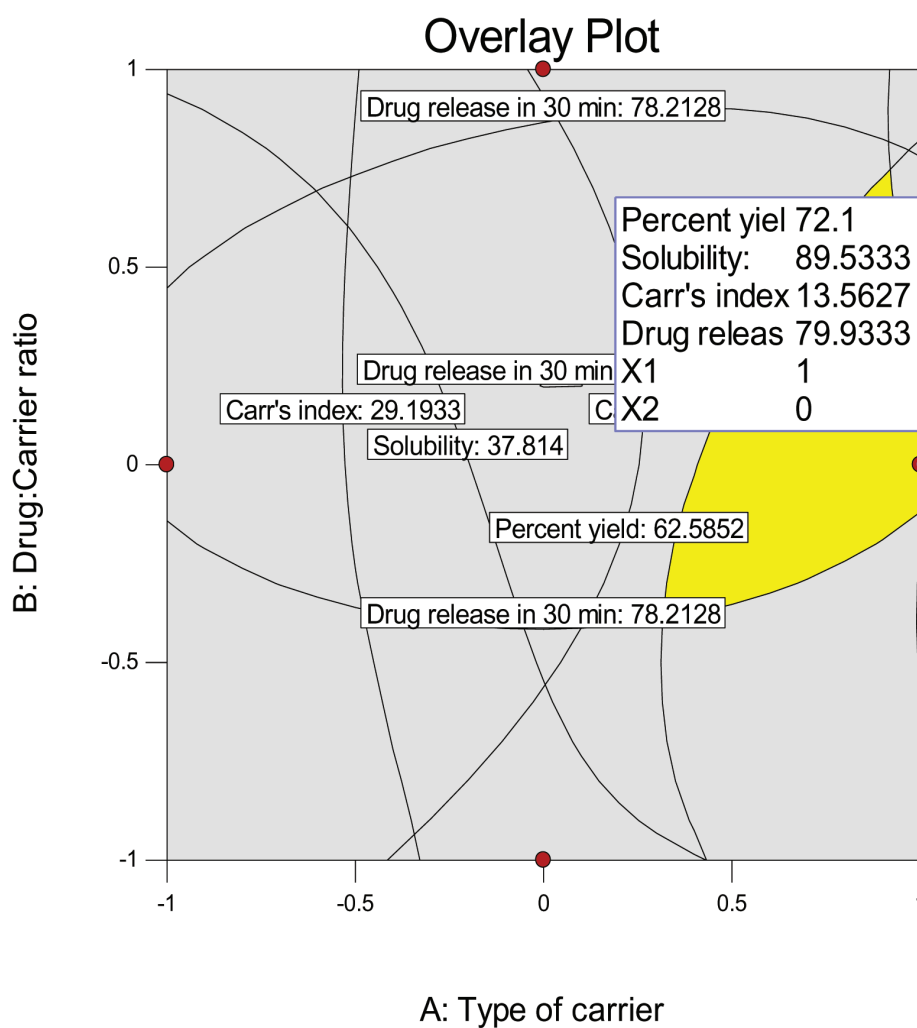


FIGURE 5 - Design space overlay plot indicating yellow color region as the design space.

CHARACTERIZATION

Solubility

The solubility data of selected inclusion complexes and polymers dispersions (F25-F36) was shown in Table V. It was observed that inclusion complexes of ramipril

with β -CD (1:4) ratio showed higher solubility (120 $\mu\text{g/ml}$) compared to other formulations. The polymer dispersions between drug and HPMC K100M (1:1) ratio showed the lowest drug solubility (12 $\mu\text{g/ml}$) among the other hydrophilic carriers. The above result indicated that complexes with β -CD improved the solubility of the selected drug to a greater extent.

TABLE V - Solubility ($\mu\text{g/ml}$), percentage yield (%), and drug content (%) data of selected inclusion complexes formulations prepared by co-evaporation method, Data expressed as mean \pm S.D. (n=6)

Formulation code	Solubility ($\mu\text{g/mL}$) (Mean \pm S.D)	Percentage yield (%) (Mean \pm S.D)	Drug content (%) (Mean \pm S.D)
F25	54 \pm 1.54	73 \pm 2.07	29.00 \pm 1.89
F26	95 \pm 1.89	71 \pm 1.23	19.00 \pm 1.45
F27	120 \pm 1.54	74.20 \pm 1.76	59.75 \pm 1.34
F28	40 \pm 1.53	70.12 \pm 1.67	44.25 \pm 1.98
F29	43 \pm 1.76	71.14 \pm 1.98	41.09 \pm 1.43
F30	48 \pm 1.22	45.26 \pm 1.74	41.29 \pm 1.98
F31	52 \pm 0.99	10.50 \pm 1.12	14.19 \pm 1.57
F32	60 \pm 1.11	48.95 \pm 2.03	22.17 \pm 2.04
F33	89 \pm 2.00	10 \pm 1.94	19.75 \pm 1.23
F34	12 \pm 1.59	55.24 \pm 2.03	39.18 \pm 2.13
F35	22 \pm 1.98	48.19 \pm 1.83	40.78 \pm 2.03
F36	26 \pm 1.23	47.20 \pm 1.43	41.79 \pm 1.78

S.D: Standard deviation; n: no of number of observations

Percentage yield

The production yield of complexes and polymers dispersions were prepared by physical mixing, kneading, co-evaporation, and solvent evaporation methods are mentioned in Table V. The most probable reason for the low percentage yield could be wastage of formulation ingredients during the preparation process.

Drug content

The drug content of all formulations has been summarized in Table V, and the drug content was found to be between 12 to 97%.

Micromeritics properties

One of the critical factors affecting the flowability of ramipril is interarticular friction. The prepared formulations exhibited the desired flowability due to the optimal presence of moisture and diminished cohesiveness. The results of flow properties such as angle of repose, carr's index, Hausner's ratio, bulk density, tapped density, and flow rate of the prepared formulations are represented in Table VI. The pure drug has an angle of repose of 45° and exhibited poor flow. In contrast, all the formulations' angles of repose showed excellent to good flowability with values ranging from 13.56 to 32.14°. The values of Carr's index of all formulations were found to

be either less than 40%, excluding formulations F3, F10, F12, and F19 having values ≥ 40 , indicating excellent flow properties as well as compressibility. However, the pure drug demonstrated poor flow property with Carr's index value of 52. Hausner's ratio of the pure drug was 3.10, which indicated poor flowability, whereas the formulated complexes exhibited good flow properties due to lower values (0.50 to 0.90). The bulk density of the pure drug was determined to be 2.15 gm/cm^3 , and the inclusion complexes demonstrated values between 0.19

and 0.92 gm/cm^3 . This indicated that the pure drug has poor flow property compared to inclusion complexes. The pure drug has a tapped density of 11 gm/cm^3 and thus exhibited poor flow. In contrast, the tapped density of all the formulations showed excellent flowability as the obtained tapped density values ranged from 0.5 to 10 gm/cm^3 . Likewise, the flow rate of all formulations ranged from 30 to 1330 mg/sec compared to the pure drug (100 mg/sec), indicating the good flow property of the complex formulations.

TABLE VI - Micromeretic properties data of pure drug and selected inclusion complexes formulations prepared by co-evaporation method, Data expressed as mean \pm S.D. (n=6)

Formulation code	Angle of repose (θ) (Mean \pm S.D)	Carr's index (%) (Mean \pm S.D)	Hausner's ratio (Mean \pm S.D)	Bulk density (gm/cm^3) (Mean \pm S.D)	Tapped density (gm/cm^3) (Mean \pm S.D)	Flow rate (mg/sec) (Mean \pm S.D)
F0	45 \pm 0.85	52 \pm 0.42	3.10 \pm 0.63	2.15 \pm 1.51	11 \pm 0.92	100 \pm 1.23
F25	21.74 \pm 0.23	39.40 \pm 0.74	0.60 \pm 1.74	0.44 \pm 1.59	2 \pm 0.59	292 \pm 1.22
F26	28.65 \pm 1.23	28.58 \pm 1.76	0.71 \pm 1.41	0.50 \pm 1.25	3 \pm 0.72	710 \pm 1.34
F27	25.41 \pm 1.21	15 \pm 0.75	0.75 \pm 1.92	0.61 \pm 1.61	4.50 \pm 0.55	1236.60 \pm 1.33
F28	14.29 \pm 0.56	28.16 \pm 0.63	0.72 \pm 0.89	0.69 \pm 1.29	2.59 \pm 0.63	824.19 \pm 1.31
F29	19.18 \pm 0.53	29.18 \pm 0.42	0.62 \pm 0.86	0.75 \pm 1.53	3.18 \pm 0.82	642.23 \pm 1.30
F30	21.07 \pm 0.87	20.16 \pm 0.63	0.61 \pm 0.98	0.81 \pm 1.32	5.78 \pm 0.86	500.12 \pm 1.29
F31	13.56 \pm 0.98	36.37 \pm 0.41	0.63 \pm 0.85	0.19 \pm 1.92	0.70 \pm 0.93	30 \pm 1.32
F32	17.06 \pm 0.32	29.17 \pm 0.49	0.56 \pm 0.84	0.24 \pm 1.83	3.29 \pm 0.74	61.28 \pm 1.31
F33	26.16 \pm 0.59	37.50 \pm 0.62	0.62 \pm 1.11	0.20 \pm 1.90	1.50 \pm 0.82	125 \pm 1.39
F34	21.09 \pm 0.93	33.46 \pm 0.83	0.75 \pm 1.21	0.65 \pm 1.62	3.18 \pm 0.93	101.45 \pm 1.09
F35	22.78 \pm 0.73	37.15 \pm 0.41	0.71 \pm 1.09	0.52 \pm 1.52	6.23 \pm 0.77	85.26 \pm 1.15
F36	27.19 \pm 0.78	24.19 \pm 0.63	0.63 \pm 1.04	0.34 \pm 1.43	3.29 \pm 0.69	245.29 \pm 1.28

S.D: Standard deviation; n: no of number of observations

***In-vitro* drug release study**

The *in-vitro* drug release studies of pure drug and all formulations were performed using phosphate buffer pH 6.8 as dissolution medium for 1h. All these formulations show faster drug release due to drug particles in the

polymeric cavity of the formed complexes and polymers dispersions by the co-evaporation method (Figure 6 A and B). The data obtained from *in-vitro* release studies were applied to various kinetic models to know the mechanism of drug release. To illustrate drug release kinetics from the formulations, release data were analyzed according

to different kinetic equations. Drug release data of all the formulations followed Higuchi kinetic model due to its higher model as regression coefficient values than other kinetic models. Further, all the formulations showed a higher correlation in Higuchi kinetics, indicating diffusion is the drug release mechanism. This is indicative of drug complex formation between the model drug and selected carriers. The data obtained were also put in Koresmeyer-

Peppas's model to determine the drug diffusion coefficient or release exponent (n). The n-value of complexes of different formulations ranged from 0.0174 to 1.0694, indicating that the drug released was diffusion controlled due to the drug's faster disintegration and dissolution rate (Table VII). Based on the above discussion, it can be observed that the formulation (F27) containing the β -CD (1:4) ratio is the best.

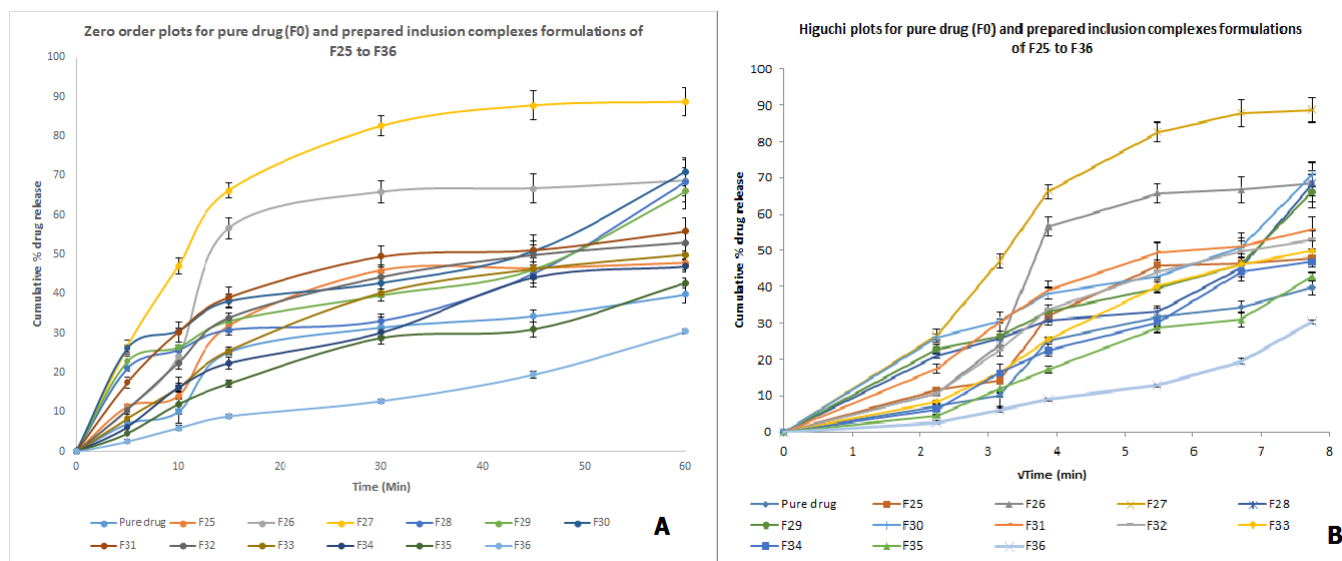


FIGURE 6 - Zero order plot for pure drug (F0), inclusion complexes and polymers dispersions (F25 to F36) [A]; and Higuchi order plot for pure drug (F0) inclusion complexes and polymers dispersions (F25 to F36) [B] by co-evaporation method.

TABLE VII - *In-vitro* dissolution kinetics data of inclusion complex of selected formulations

Formulation code	Zero order plot	First order plot	Higuchi plot	Koresmeyer-Peppas's plot	
		R ²		n	
F0	0.8596	0.8933	0.9371	0.9509	0.903
F25	0.8011	0.8324	0.9154	0.9230	0.9411
F26	0.7246	0.8324	0.8626	0.9142	1.0495
F27	0.7478	0.9094	0.9272	0.8444	1.0426
F28	0.8879	0.9438	0.9634	0.8436	0.8197
F29	0.8793	0.9873	0.9947	0.8938	0.8234
F30	0.8535	0.9584	0.9452	0.8832	0.8647
F31	0.7315	0.8439	0.8569	0.8551	0.9291
F32	0.8409	0.9745	0.9829	0.8945	0.9120
F33	0.9052	0.9439	0.9706	0.9585	0.9559

TABLE VII - *In-vitro* dissolution kinetics data of inclusion complex of selected formulations

Formulation code	Zero order plot	First order plot	Higuchi plot	Koresmeyer-Peppas's plot	
	R ²			n	
F34	0.9383	0.9458	0.9625	0.8352	0.8214
F35	0.9520	0.9850	0.9780	0.8950	0.8457
F36	0.9799	0.9787	0.9945	0.8975	0.8761

R²: Regression correlation coefficient; n: Diffusion exponent coefficient

Stability study

The stability study for the F27 formulation was performed by studying the formulation's drug content and release before and after the stress condition. Short-term stability studies as per ICH guidelines were carried out for the F27 formulation. The drug content and the cumulative percentage of drug release data are mentioned

in Table VIII. After three months of stability study (before and after storage), it was observed that the formulation (F27) remained stable even after exposure to a higher temperature. Statistically, no significant differences were observed in drug content ($p < 0.05$, $F_{cal}=0.1541$ and $F_{crit}=6.2412$), as well as *in-vitro* drug release ($p < 0.05$, $F_{cal}=2.4329$ and $F_{crit}=7.6999$).

TABLE VIII - Stability data of the optimized batch formulation (F27) on before and after storage conditions

Formulation	Before stability		After stability	
	Drug content (%)* (Mean ± S.D)	Cumulative drug release (%)* (Mean ± S.D)	Drug content (%)* (Mean ± S.D)	Cumulative drug release (%)* (Mean ± S.D)
F27	59.75±0.09	88.74±0.12	60.02±0.56	88.45±0.03

*Mean ± S.D, n=6; S.D: Standard deviation; n: Number of observations

CONCLUSION

The inclusion complexes of ramipril with β-cyclodextrin (1:4) prepared by the co-evaporation method showed the highest solubility and fast dissolution profile as per other ways with the application of I-optimal experimental design. FT-IR, DSC, and X-RD studies revealed no interaction between drug and polymer. It means that there were no changes in the drug and carrier properties during the preparation of inclusion complexes, and both drug and polymer are compatible with each other. The *in-vitro* drug release kinetics of the

complex formulation showed Higuchi release kinetics as a regression correlation more than different release kinetics ($R^2=0.9272$). As per ICH guidelines for F27 formulation, stability studies showed no significant change in drug content and drug release data after three months' storage condition, and it is stable. From the present investigation, it can be concluded that such an inclusion complex of ramipril may help manage hypertension by reducing drug administration frequency and the right way to bypass the extensive hepatic first-pass metabolism of the drug by improving solubility and dissolution rate of the selected model drug.

DECLARATIONS

The ethical approval and consent to participate:
Non-applicable.

CONSENT FOR PUBLICATION

All the authors have given their consent for publishing this manuscript.

AVAILABILITY OF DATA AND MATERIAL

Non-applicable.

COMPETING INTERESTS

The author declares there are no conflicts of notice in preparing the manuscript.

FUNDING

No funding was received.

AUTHORS' CONTRIBUTIONS

“All authors have read and approved the manuscript.” Each author is expected to have made substantial contributions to the conception or design of the manuscript; or the acquisition, drafting, and language editing or substantively revised it and to have approved the submitted version (and any substantially modified version that involves the author's contribution to the study); and to have agreed both to be personally accountable for the author's gifts and to ensure that questions related to the accuracy or integrity of any part of the work, even ones in which the author was not personally involved, are appropriately investigated, resolved, and the resolution documented in the literature.

ACKNOWLEDGEMENTS

The authors are thankful to the School of Pharmacy and Medical Sciences, Singhania University, Pacheri Bari, Jhunjhunu, Rajasthan-333 515, India, for their

ever and tireless encouragement, support, and providing research environment.

REFERENCES

Alderman MH. Hypertension control: improved, but not enough! *Am J Hypertens.* 2007;20(4):347.

Aleksandra Z, Nuno R, Alessandra D, Massimo L, Nicola C, Soukaina EM, et al. Development and optimization of alpha-pinene-loaded solid lipid nanoparticles (SLN) using experimental factorial design and dispersion analysis. *Molecules.* 2019;24(15):2683.

Chobanian AV, Bakris GL, Black HR, Cushman WC, Green LA, Izzo JL Jr, et al. Seventh report of the joint national committee on prevention, detection, evaluation, and treatment of high blood pressure. *Hypertension.* 2003;42(6):1206-1252.

Duchene D, Wouessidjewe D. Pharmaceutical uses of cyclodextrins and derivatives. *Drug Dev Ind Pharm.* 1990;16(17):2487-2499.

Ekambaram P, Abdul HS. Formulation and evaluation of solid lipid nanoparticles of ramipril. *J Young Pharm.* 2011;3(3):216-20.

Higuchi T, Connors KA. Phase solubility techniques. *Adv Anal Chem Instrum.* 1965;4:117-212.

Kedzierzewicz F, Huffman M, Maincent P. Comparison of tolbutamide β -cyclodextrin inclusion compounds and solid dispersions: Physicochemical characteristics and dissolution studies. *Int J Pharm.* 1990;58(3):221-227.

Kim CK, Choi JY, Yoon YS, Gong JP, Choi HG, Kong JY, et al. Preparation and evaluation of a dry elixir for the enhancement of the dissolution rate of poorly water-soluble drugs. *Int J Pharm.* 1994;106(1):25-32.

Kislalioglu MS, Khan MA, Blount C, Goettsch RW, Bolton S. Physical characterization and dissolution properties of ibuprofen: Eudragit coprecipitates. *J Pharm Sci.* 1991;80(8):799-804.

Komati S, Swain S, Rao MEB, Jena BR, Dasi V. QbD-based design and characterization of mucoadhesive microspheres of quetiapine fumarate with improved oral bioavailability and brain biodistribution potential. *Bull Fac Pharm Cairo Univ.* 2018;56(2):129-145.

Mukherjee S, Ray S, Thakur RS. Solid lipid nanoparticles: A modern formulation approach in drug delivery system. *Indian J Pharm Sci.* 2009;71(4):349-58.

Muller RH, Mader K, Gohla S. Solid lipid nanoparticles (SLN) for controlled drug delivery-A review of the state of the art. *Eur J Pharm Biopharm.* 2000;50(1):161-77.

Nambu N, Kikuchi K, Kikuchi T, Takahashi Y, Ueda H, Nagai T. Influence of inclusion of nonsteroidal antiinflammatory drugs with β -cyclodextrin on the irritation to stomach of rats upon oral administration. *Chem Pharm Bull.* 1978;26(12):3609-3612.

Parhi R, Reddy SS, Swain S. Transdermal delivery of ondansetron HCl from thermoreversible gel containing nanocomposite. *Curr Nanometer.* 2019;4(2):137-147.

Parhi R, Suresh P, Pattnaik S. Pluronic lecithin organogel (PLO) of diltiazem hydrochloride: effect of solvents/penetration enhancers on ex-vivo permeation. *Drug Deliv Transl Res.* 2016;6(3):243-253.

Patra CN, Swain S, Mohanty S, Panigrahi KC. Design and characterization of aceclofenac and paracetamol spherical crystals and their tableting properties. *Powder Technol.* 2015;274:446-454.

Rao MEB, Swain S, Patra CN, Jammula S, Patra S. Development and in vitro evaluation of floating multiparticulate system of repaglinide. *FABAD J Pharm Sci.* 2011;36(2):75-92.

Sugawara M, Kadomura S, Xin H, Takekuma Y, Khori N, Miyazaki K. The use of an in vitro dissolution and absorption system to evaluate oral absorption of two weak bases in pH-independent controlled-release formulations. *Eur J Pharm Sci.* 2005;26(1):1-8.

Swain S, Behera A, Dinda SC, Patra CN, Jammula S, Beg S, et al. Formulation design, optimization and pharmacodynamic evaluation of sustained release mucoadhesive microcapsules of venlafaxine HCl. *Indian J Pharm Sci.* 2014;76(4):267-378.

Swain S, Behera UA, Beg S, Sruti J, Patro CN, Dinda SC, et al. Design and characterization of enteric-coated controlled release mucoadhesive microcapsules of rabeprazole sodium. *Drug Dev Ind Pharm.* 2012;39(4):548-60.

Swain S, Sahu PK, Jena BR, Beg S, Babu SM. Formulation development, statistical optimization and characterization of the self-microemulsifying drug delivery system (SMEDDS) of irbesartan. *Nanosci Nanotechnol-Asia.* 2019;9(2):210-228.

Szejtli J. Cyclodextrin in drug formulations: Part II. *Pharm Tech.* 1991;24-38.

Yoshida A, Arima H, Uekama K, Pitha J. Pharmaceutical evaluation of hydroxyalkyl ethers of β -cyclodextrin. *Int J Pharm.* 1988;46(3):217-222.

Youn YS, Tung JYS, Yoo SD, Lee KC. Improved intestinal delivery of salmon calcitonin by Lys18-amine specific PEGylation: Stability, permeability, pharmacokinetic behavior and in vivo hypocalcemic efficacy. *J Contr Rel.* 2006;144(3):334-42.

Received for publication on 21st March 2021
Accepted for publication on 29th August 2021